

---

*Supplementary Materials*

# **Aqueous 2-Ethyl-4-methylimidazole Solution for Efficient CO<sub>2</sub> Separation and Purification**

**Xingtian Zhang<sup>1,2,3</sup>, Jun Wu<sup>4</sup>, Xiaoxiao Lu<sup>3</sup>, Yefeng Yang<sup>1,\*</sup>, Li Gu<sup>2,\*</sup> and Xuebo Cao<sup>3,\*</sup>**

<sup>1</sup> School of Materials Science and Engineering, Zhejiang Sci-Tech University, Hangzhou 310018, China.

<sup>2</sup> School of Materials and Textile Engineering, Jiaying University, Jiaying, Zhejiang 314001, China.

<sup>3</sup> College of Biological, Chemical Sciences and Engineering, Jiaying University, Jiaying, Zhejiang 314001, China.

<sup>4</sup> College of Advanced Materials Engineering, Jiaying Nanhu University. Jiaying, Zhejiang 314001, China.

\* Correspondence: yangyf@zstu.edu.cn; guli@zjxu.edu.cn; xbcao@zjxu.edu.cn; Tel.: +86-0573-83642712

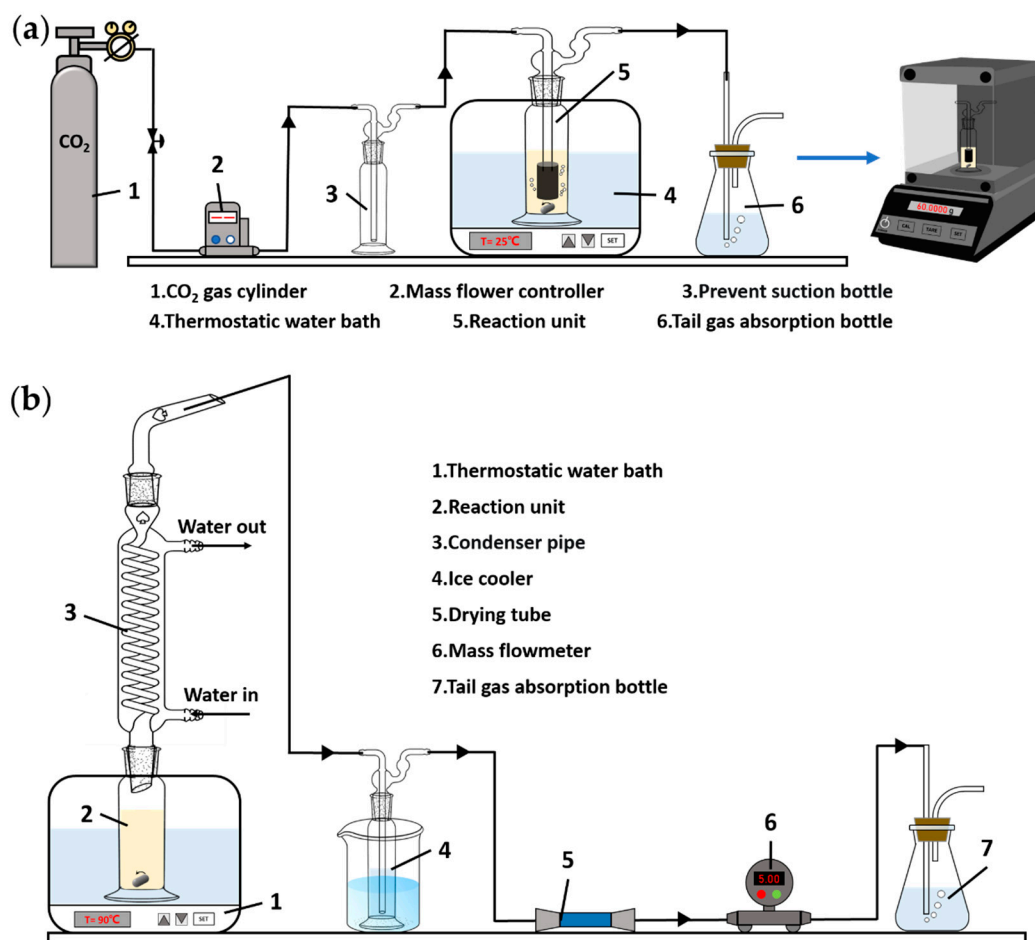


**Figure S1.** Schematic of experimental setups. (a) CO<sub>2</sub> absorption setup. (b) CO<sub>2</sub> desorption setup.

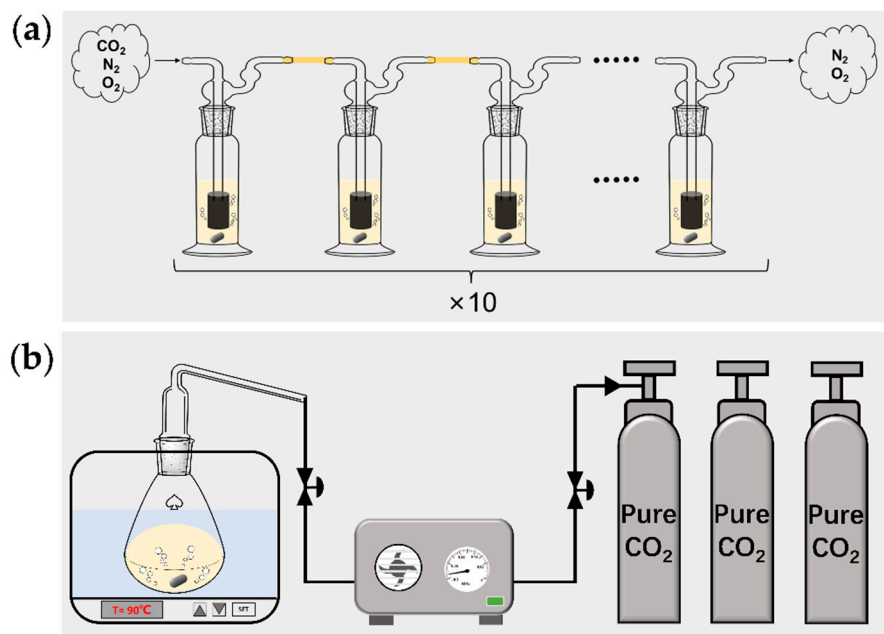


**Figure S2.** (a) Schematic of the bubbling absorption setup, which consists of 10 bubbling reactors connected in series. (b) Schematic of desorption and compression setup.

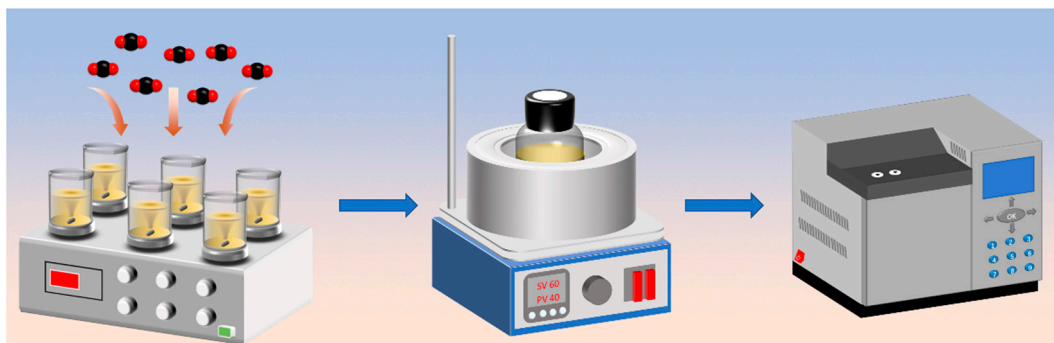


**Figure S3.** Schematic of imidazole aqueous solution direct air capture and heat concentration of CO<sub>2</sub>.

---

**Table S1** Basic properties of ten solid imidazoles.

Compounds	Molecular formula	Molecular weight	Density	Melting point	Boiling point (at 760 mmHg)	Vapour pressure (at 25°C)	pKa (at 25°C)
Imidazole	C <sub>3</sub> H <sub>4</sub> N <sub>2</sub>	68.08	1.01 g/mL	90-91 °C	257 °C	0.024 mmHg	6.95
2-Methylimidazole	C <sub>4</sub> H <sub>6</sub> N <sub>2</sub>	82.10	1.06 g/mL	142-145 °C	267 °C	0.014 mmHg	7.85
4-Methylimidazole	C <sub>4</sub> H <sub>6</sub> N <sub>2</sub>	82.10	1.02 g/mL	44-47 °C	263 °C	0.017 mmHg	7.69
2-Ethylimidazole	C <sub>5</sub> H <sub>8</sub> N <sub>2</sub>	96.13	1.02 g/mL	78-80 °C	268 °C	0.013 mmHg	7.99
2-Propylimidazole	C <sub>6</sub> H <sub>10</sub> N <sub>2</sub>	110.16	0.99 g/mL	56-62 °C	286 °C	0.005 mmHg	8.02
2-Buthylimidazole	C <sub>7</sub> H <sub>12</sub> N <sub>2</sub>	124.18	0.98 g/mL	52 °C	279 °C	0.007 mmHg	8.00
2-Isopropylimidazole	C <sub>6</sub> H <sub>10</sub> N <sub>2</sub>	110.16	0.99 g/mL	129-131 °C	258 °C	0.0227 mmHg	7.97
1,2-Dimethylimidazole	C <sub>5</sub> H <sub>8</sub> N <sub>2</sub>	96.13	1.08 g/mL	29-30 °C	206 °C	0.348 mmHg	8.21
2,4-Dimethylimidazole	C <sub>5</sub> H <sub>8</sub> N <sub>2</sub>	96.13	0.97 g/mL	85-87 °C	274 °C	0.010 mmHg	8.50
2-Ethyl-4-methylimidazole	C <sub>6</sub> H <sub>10</sub> N <sub>2</sub>	110.16	0.98 g/mL	47-54 °C	276 °C	0.008 mmHg	8.68

**Table S2** Summary of CO<sub>2</sub> capture capacity of various imidazole aqueous solutions.

Compounds	Concentration	CO <sub>2</sub> capture capacity	Ref.
Imidazole	3 M	0.19 mol/mol	1
1-Methylimidazole	3 M	0.13 mol/mol	1
2-Methylimidazole	3 M	0.42 mol/mol	1
4-Methylimidazole	3 M	0.31 mol/mol	1
1,2-Dimethylimidazole	3 M	0.35 mol/mol	1
Imidazole	30 wt%	0.21 mol/mol	2
1-Methylimidazole	30 wt%	0.12 mol/mol	2
2-Methylimidazole	30 wt%	0.36 mol/mol	2
4-Methylimidazole	30 wt%	0.29 mol/mol	2
2-Ethylimidazole	30 wt%	0.29 mol/mol	2
1,2-Dimethylimidazole	30 wt%	0.36 mol/mol	2
2-Ethyl-4-methylimidazole	30 wt%	0.47 mol/mol	2
Imidazole	6.67 wt%	0.45 mol/mol	This work
2-Methylimidazole	6.67 wt%	0.80 mol/mol	This work
4-Methylimidazole	6.67 wt%	0.67 mol/mol	This work
2-Ethylimidazole	6.67 wt%	0.79 mol/mol	This work
2-Propylimidazole	6.67 wt%	0.78 mol/mol	This work
2-Buthylimidazole	6.67 wt%	0.74 mol/mol	This work
2-Isopropylimidazole	6.67 wt%	0.75 mol/mol	This work
1,2-Dimethylimidazole	6.67 wt%	0.82 mol/mol	This work
2,4-Dimethylimidazole	6.67 wt%	0.85 mol/mol	This work
2-Ethyl-4-methylimidazole	3.33 wt%	1.01 mol/mol	This work
2-Ethyl-4-methylimidazole	6.67 wt%	0.88 mol/mol	This work
2-Ethyl-4-methylimidazole	13.33 wt%	0.80 mol/mol	This work
2-Ethyl-4-methylimidazole	20.00 wt%	0.69 mol/mol	This work

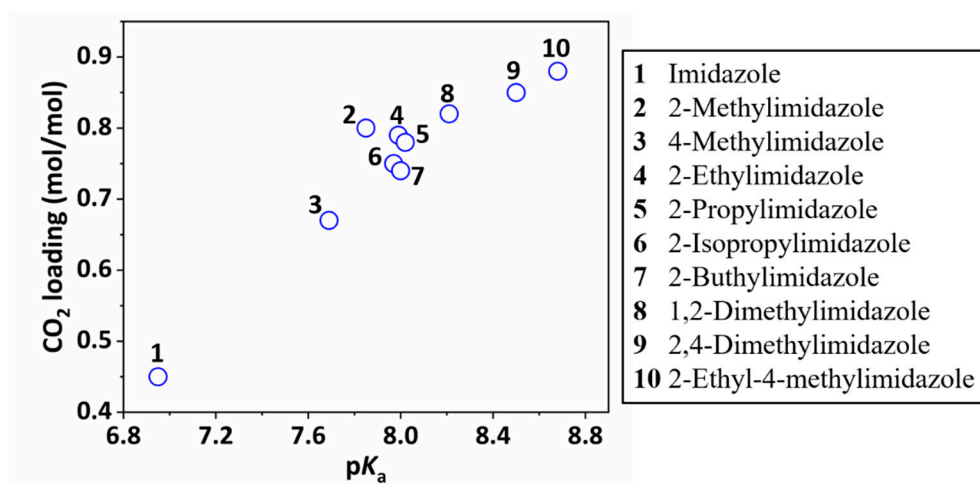
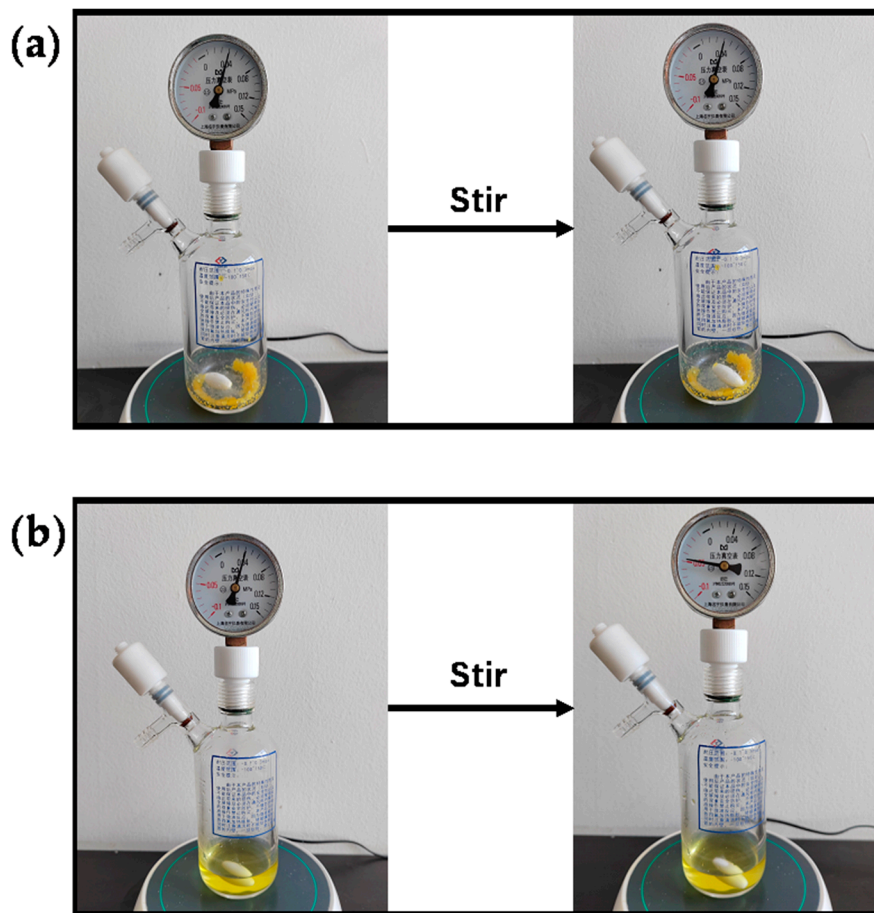


**Figure S4.** Relationship between molar absorption of  $\text{CO}_2$  and  $\text{pK}_a$ .

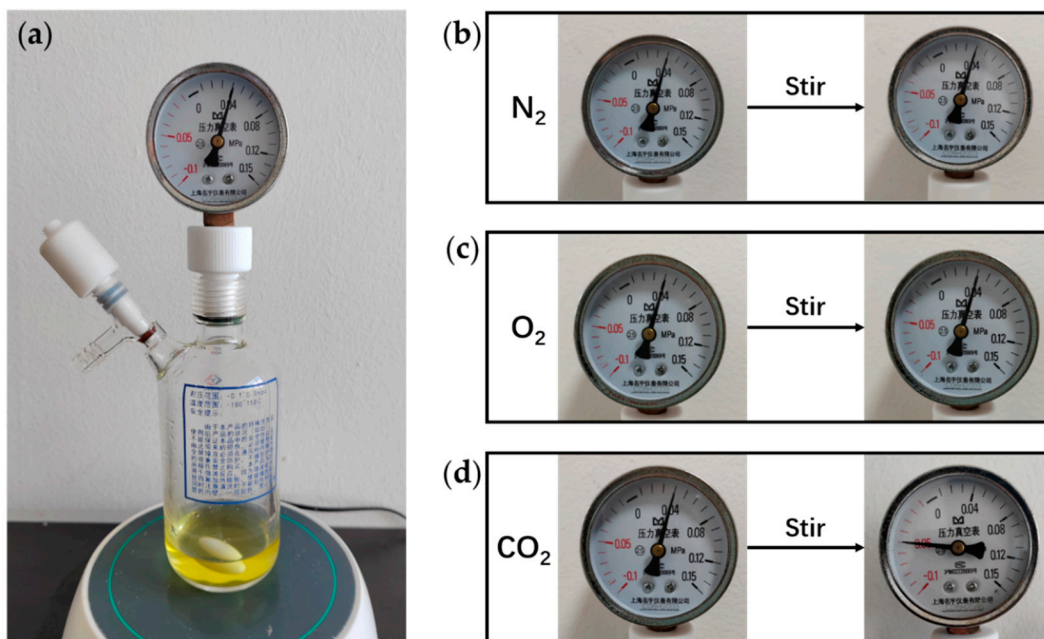


\*压力真空表: pressure vacuum gauge

**Figure S5.** Study on CO<sub>2</sub> absorption capacity of 2-ethyl-4-methylimidazole by using anhydrous solid and aqueous solution. (a) Photographs showing the absorption of CO<sub>2</sub> by pure 2-ethyl-4-methylimidazole solid. (b) Photographs showing the absorption of CO<sub>2</sub> by 2-ethyl-4-methylimidazole aqueous solution.

The pressure gauge can indicate the change of gas pressure in the pressure-resistant reaction bottle. Before the reaction, the bottle was vacuumized, filled with CO<sub>2</sub> gas to a pressure of 0.04 MPa, and then stirred for absorption. The experiment shows that the pointer of the bottle containing pure 2-ethyl-4-methylimidazole solid keeps a reading of 0.04 MPa, while the pointer of the bottle containing 2-ethyl-4-methylimidazole aqueous solution drops from 0.04 MPa to about -0.05 MPa.





\*压力真空表: pressure vacuum gauge

**Figure S6.** Study on selective gas absorption. (a) Photograph of reaction experiment setup. (b-d) Photographs showing that the reading of the pressure gauge pointer changes under different gas feeds. (b) N<sub>2</sub>, (c) O<sub>2</sub>, (d) CO<sub>2</sub>.

Add 2-ethyl-4-methylimidazole aqueous solution into a pressure resistant reaction bottle, and vacuum the gas before reaction. Inject high-purity N<sub>2</sub>, O<sub>2</sub> and CO<sub>2</sub> gas into the bottle to make the pressure in the bottle reach about 0.04 Mpa, and then stir for absorption. It can be seen that the pointer reading of the bottle filled with N<sub>2</sub> and O<sub>2</sub> is maintained at 0.04 Mpa.

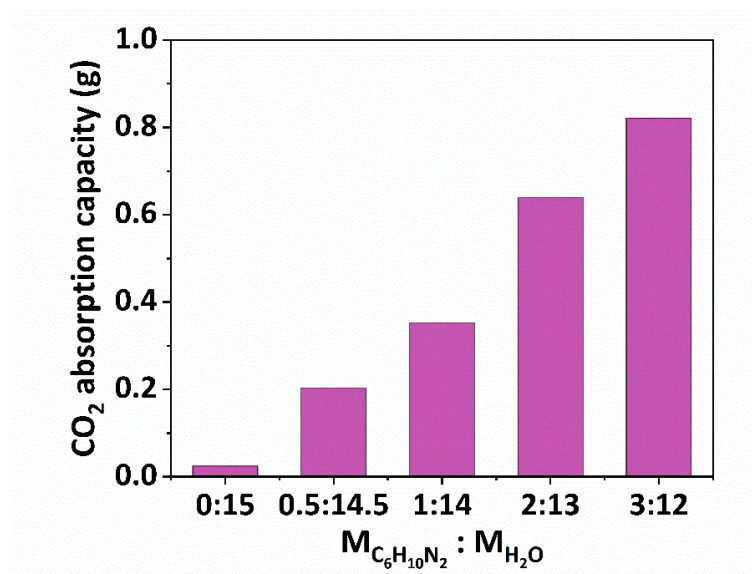


**Figure S7.** CO<sub>2</sub> absorption capacity of 2-ethyl-4-methylimidazole solution with different mass fractions.

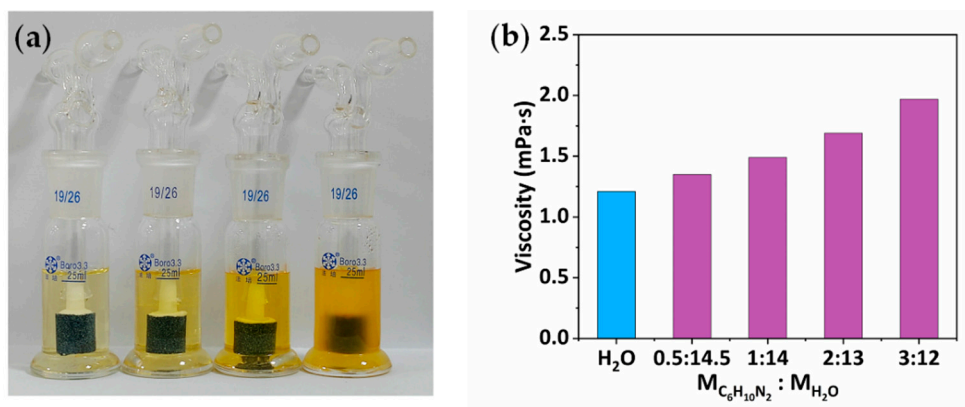


**Figure S8.** (a) Photograph of 2-ethyl-4-methylimidazole solution with different mass fractions. (b) Viscosities of various 2-ethyl-4-methylimidazole solutions.

**Table S3** Comparison of 2-ethyl-4-methylimidazole and amine absorbents.

Absorbent	Absorption gas composition	CO <sub>2</sub> capture capacity	Desorption temperature	Ref.
DBA + H <sub>2</sub> O + ethanol	pure CO <sub>2</sub>	0.82 mol/mol	100 °C	3
DMCA + MCA + H <sub>2</sub> O	pure CO <sub>2</sub>	0.985 mol/mol	110 °C	4
AMP + PZ + DME	pure CO <sub>2</sub>	0.87 mol/mol	120 °C	5
EMEA + DEEA	pure CO <sub>2</sub>	0.677 mol/mol	110 °C	6
MEA + sulfolane + H <sub>2</sub> O	15% CO <sub>2</sub> 85% N <sub>2</sub>	0.518 mol/mol	120 °C	7
[NH <sub>2</sub> e-mim][BF <sub>4</sub> ] + MEA+ H <sub>2</sub> O	pure CO <sub>2</sub>	0.4554 mol/mol	120 °C	8
AMP + PZ + MEA+ H <sub>2</sub> O	15% CO <sub>2</sub> 85% N <sub>2</sub>	0.61 mol/mol	90 °C	9
DEEA + AEEA + H <sub>2</sub> O	12% CO <sub>2</sub> 88% N <sub>2</sub>	0.64 mol/mol	120 °C	10
MEA + AMP + DMSO + PMDETA	pure CO <sub>2</sub>	0.88 mol/mol	120 °C	11
EMEA + DEEA + PX	pure CO <sub>2</sub>	0.59 mol/mol	100 °C	12
TETA + AMP + NMF	15% CO <sub>2</sub> 85% N <sub>2</sub>	0.86 mol/mol	120 °C	13
2-Ethyl-4-methylimidazole + H <sub>2</sub> O	pure CO <sub>2</sub>	0.80 mol/mol	90 °C	This work
2-Ethyl-4-methylimidazole + H <sub>2</sub> O	15% CO <sub>2</sub> 8% O <sub>2</sub> 77% N <sub>2</sub>	0.54 mol/mol	90 °C	This work

**DBA:** dibutylamine, **DMCA:** *N,N*-dimethylcyclohexylamine, **MCA:** *N*-methylcyclohexylamine, **AMP:** 2-amino-2-methyl-1-propanol, **PZ:** piperazine, **DME:** dipropylene glycol dimethyl ether, **EMEA:** *N*-ethylmonoethanolamine, **DEEA:** *N,N*-diethylethanolamine, **MEA:** monoethanolamine, **[NH<sub>2</sub>e-mim][BF<sub>4</sub>]:** (1-(1-aminoethyl)-3-methylimidazole fluoroborate, **AEEA:** 2-((2-aminoethyl) amino) ethanol, **DMSO:** dimethyl sulfoxide, **TETA:** triethylene tetramine, **PX:** *p*-xylene, **PMDETA:** *N,N,N',N'',N'''*-pentamethyldiethylenetriamine, **NMF:** *N*-methylformamide.

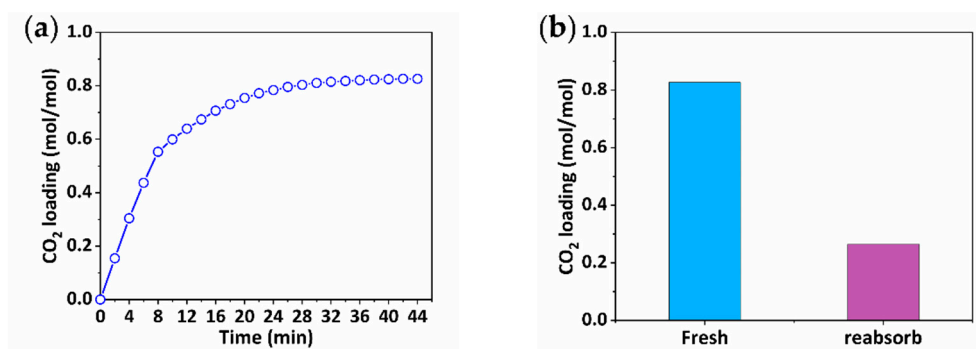


**Figure S9.** CO<sub>2</sub> absorption-desorption performance of ethanolamine. (a) Absorption capacity curve of ethanolamine with time (2 g MEA + 13 mL H<sub>2</sub>O). (b) After desorption at 90 °C, the secondary reabsorption rate of MEA significantly decreases.

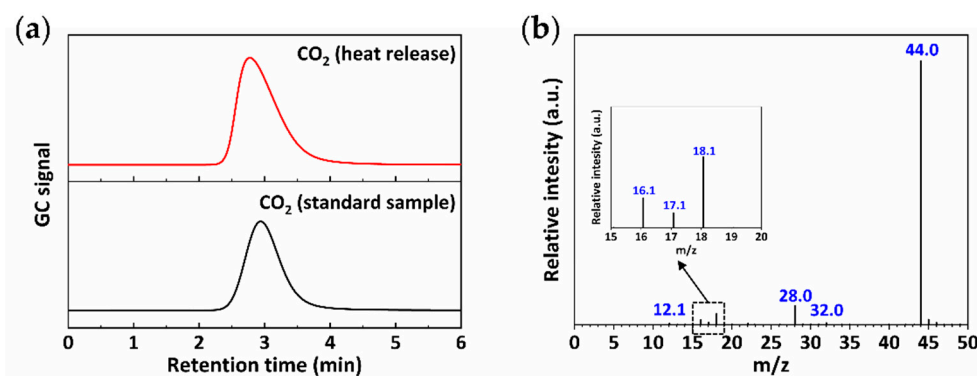


**Figure S10.** (a) Gas chromatography measurements of heat released gas. (b) Mass spectrum of heat released gas.

In order to verify the accuracy of the GC signal, standard CO<sub>2</sub> was tested, and the GC curve (black line) was recorded for comparison. As seen, the GC signal of the released gas is identical to that of standard CO<sub>2</sub>, confirming that CO<sub>2</sub> is desorbed.

In a mass spectrometer, CO<sub>2</sub> molecules can be ionized or even split into charged fragments, such as [CO<sub>2</sub>]<sup>+</sup>, [O<sub>2</sub>]<sup>+</sup>, [CO]<sup>+</sup>, [O]<sup>+</sup> and [C]<sup>+</sup>. Fragment signal distribution is as follows: m/z=12.1, [C]<sup>+</sup>; m/z=16.1, [O]<sup>+</sup>; m/z = 28.0, [CO]<sup>+</sup>; m/z = 32.0, [O<sub>2</sub>]<sup>+</sup>; m/z = 44.0, [CO<sub>2</sub>]<sup>+</sup>. At the same time, due to a small amount of H<sub>2</sub>O in the released gas, there is m/z=16.1, [O]<sup>+</sup>; m/z=17.1, [OH]<sup>+</sup>; M/z=18.1, [H<sub>2</sub>O]<sup>+</sup> weak segment signal.

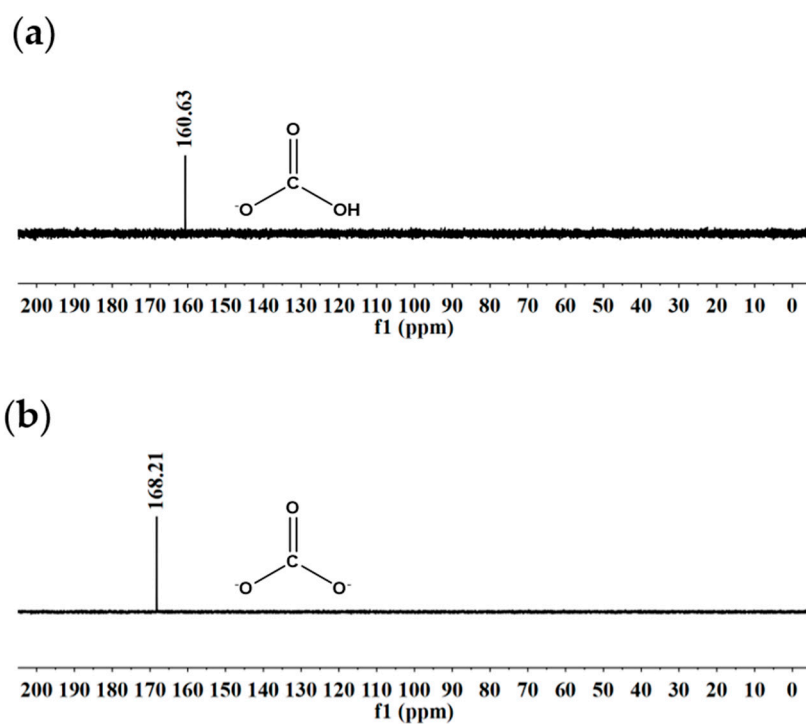


**Figure S11.** (a)  $^{13}\text{C}$  NMR spectrum of  $\text{NaHCO}_3$  aqueous solution. (b)  $^{13}\text{C}$  NMR spectrum of  $\text{NaCO}_3$  aqueous solution.

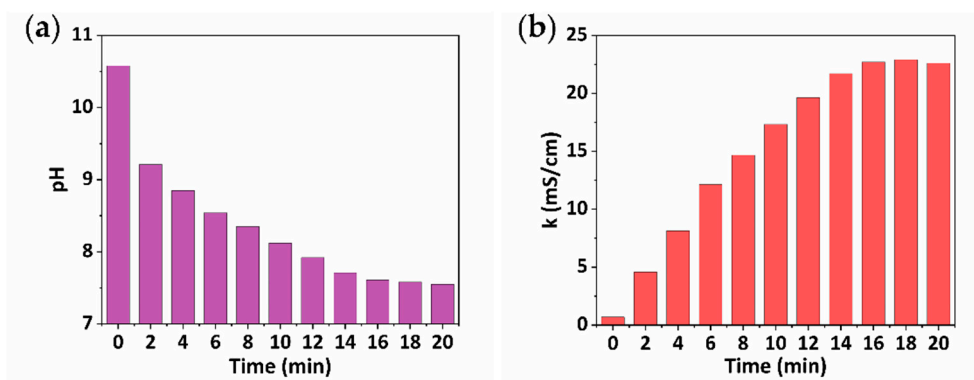


**Figure S12.** Changes of pH value and conductivity with time during CO<sub>2</sub> absorption by 2-ethyl-4-methylimidazole aqueous solution. (a) pH change. (b) Conductivity change.

It is worth noting that the initial conductivity of the solution is only 691  $\mu\text{S}/\text{cm}$ , the conductivity increases rapidly after CO<sub>2</sub> is introduced, and the conductivity after absorption saturation is 22.7 mS/cm, about 33 times of the initial conductivity value. It shows that there is only a small amount of OH<sup>-</sup> in the reaction between 2-Ethyl-4-methylimidazole and water in the initial solution, but when CO<sub>2</sub> is introduced, a large number of bicarbonate ions form and the reaction balance moves to the right, generating more OH<sup>-</sup> for CO<sub>2</sub> absorption.



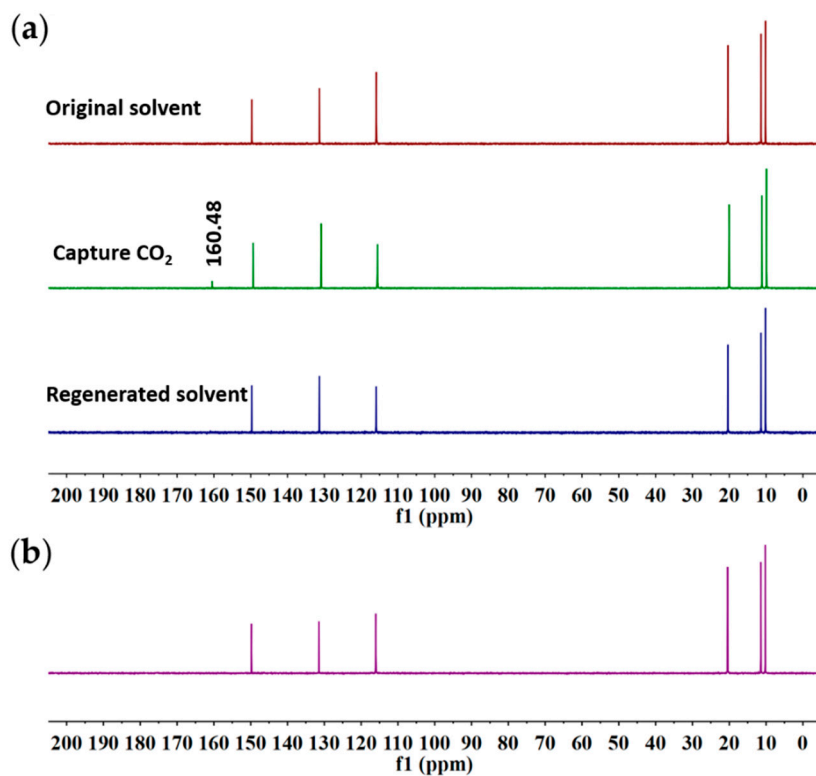


**Figure S13.** (a) <sup>13</sup>C NMR spectra of 2-ethyl-4-methylimidazole during absorption-desorption of CO<sub>2</sub> from the synthetic flue gas. (b) <sup>13</sup>C NMR spectrum of 2-ethyl-4-methylimidazole after 8 cycles.

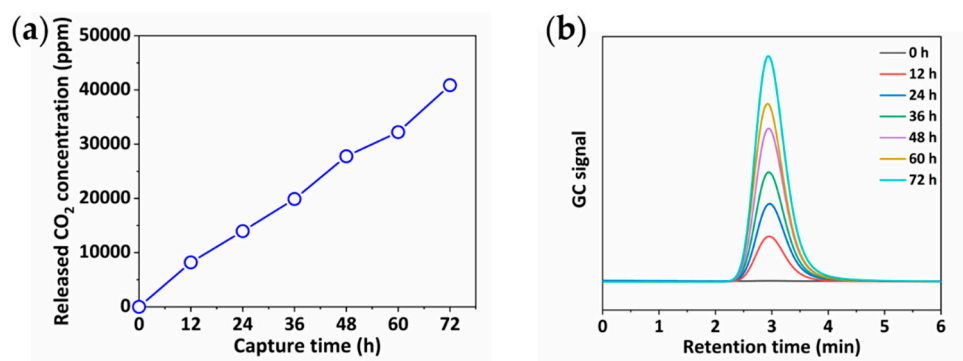


**Figure S14.** The capture of ambient air by 2-ethyl-4-methylimidazole. (a) Curve of CO<sub>2</sub> enrichment concentration with capture time. (b) Corresponds to the change of peak area detected by gas chromatography.

- 
1. Tomizaki, K.; Shimizu S.; Onoda M.; Fujioka Y. Heats of Reaction and Vapor-Liquid Equilibria of Novel Chemical Absorbents for Absorption/Recovery of Pressurized Carbon Dioxide in Integrated Coal Gasification Combined Cycle-Carbon Capture and Storage Process. *Ind. Eng. Chem. Res.* **2010**, *49*, 1214–1221.
  2. Evjen, S.; Fiksdahl, A.; Pinto, D. D. D.; Knuutila, H. K. New polyalkylated imidazoles tailored for carbon dioxide capture. *Int. J. Greenh. Gas Control.* **2018**, *76*, 167-174.
  3. Jing, G.; Liu, F.; Lv, B.; Zhou, X.; Zhou, Z. Novel Ternary Absorbent: Dibutylamine Aqueous–Organic Solution for CO<sub>2</sub> Capture. *Energy Fuels* **2017**, *31*, 12530-12539.
  4. Wang, R.; Liu, S.; Li, Q.; Zhang, S.; Wang, L.; An, S. CO<sub>2</sub> capture performance and mechanism of blended amine solvents regulated by N-methylcyclohexylamine. *Energy* **2021**, *215*, 119209-119217.
  5. Chen, Z.; Jing, G.; Lv, B.; Zhou, Z. An Efficient Solid–Liquid Biphasic Solvent for CO<sub>2</sub> Capture: Crystalline Powder Product and Low Heat Duty. *ACS Sustainable Chem. Eng.* **2020**, *8*, 14493-14503.
  6. Chen, S.; Chen, S.; Fei, X.; Zhang, Y.; Qin, L. Solubility and Characterization of CO<sub>2</sub> in 40 mass % N-Ethylmonoethanolamine Solutions: Explorations for an Efficient Nonaqueous Solution. *Ind. Eng. Chem. Res.* **2015**, *54*, 7212-7218.
  7. Liu, S.; Ling, H.; Lv, J.; Gao, H.; Na, Y.; Liang, Z. New Insights and Assessment of Primary Alkanolamine/Sulfolane Biphasic Solutions for Post-combustion CO<sub>2</sub> Capture: Absorption, Desorption, Phase Separation, and Technological Process. *Ind. Eng. Chem. Res.* **2019**, *58*, 20461-20471.
  8. Wang, M.; Wang, M.; Rao, N.; Li, J.; Li, J. Enhancement of CO<sub>2</sub> capture performance of aqueous MEA by mixing with [NH<sub>2</sub>e-mim][BF<sub>4</sub>]. *RSC Adv.* **2018**, *8*, 1987-1992.
  9. Nwaoha, C.; Saiwan, C.; Tontiwachwuthikul, P.; Supap, T.; Rongwong, W.; Idem, R.; Al-Marri, M. J.; Benamor, A. Carbon dioxide (CO<sub>2</sub>) capture: Absorption-desorption capabilities of 2-amino-2-methyl-1-propanol (AMP), piperazine (PZ) and monoethanolamine (MEA) tri-solvent blends. *J. Nat. Gas Sci. Eng.* **2016**, *33*, 742-750.
  10. Liu, F.; Fang, M.; Dong, W.; Wang, T.; Xia, Z.; Wang, Q.; Luo, Z. Carbon dioxide absorption in aqueous alkanolamine blends for biphasic solvents screening and evaluation. *Appl. Energy* **2019**, *233-234*, 468-477.
  11. Li, X.; Zhou, X.; Wei, J.; Fan, Y.; Liao, L.; Wang, H. Reducing the energy penalty and corrosion of carbon dioxide capture using a novel nonaqueous monoethanolamine-based biphasic solvent. *Sep. Purif. Technol.* **2021**, *265*, 118481-118488.
  12. Bai, L.; Lu, S.; Zhao, Q.; Chen, L.; Jiang, Y.; Jia, C.; Chen, S. Low-energy-consuming CO<sub>2</sub> capture by liquid–liquid biphasic absorbents of EMEA/DEEA/PX. *Chem. Eng. J.* **2022**, *450*, 138490-138500.
  13. Gao, X.; Li, X.; Cheng, S.; Lv, B.; Jing, G.; Zhou, Z. A novel solid–liquid ‘phase controllable’ biphasic amine absorbent for CO<sub>2</sub> capture. *Chem. Eng. J.* **2022**, *430*, 132932-132943.